INC-40007-135

Heating of Nuclear Matter and Multifragmentation: Antiprotons vs. Pions

L. Beaulieu, T. Lefort, W.-c. Hsi, K. Kwiatkowski[1], V.E. Viola,
Department of Chemistry and IUCF, Indiana University, Bloomington, IN 47405, USA

L. Pienkowski
Heavy Ion Laboratory, Warsaw University, Warsaw Poland

R.G. Korteling,
Department of Chemistry, Simon Fraser University, Burnaby, B.C., V5A 1S6 Canada

R. Laforest, E. Martin, E. Ramakrishnan, D. Rowland, A. Ruangma, E. Winchester, S.J. Yennello
Department of Chemistry and Cyclotron Institute
Texas A & M University, College Station, TX 77843

H. Breuer
Department of Physics, University of Maryland, College Park, MD 20740

S. Gushue and L.P. Remsberg
Physics Division Brookhaven National Laboratory, Upton, NY 11973

B. Back
Physics Division, Argonne National Laboratory, Argonne, IL 60439

[To be published in *Proceedings of the 15th Winter Workshop on Nuclear Dynamics,* Park City, UT, Jan. 9-16, 1999.]

*Research supported by the U.S. Department of Energy and National Science Foundation, the National Sciences and Engineering Research Council of Canada, the Robert A. Welch Foundation and Grant No. P03B 048 15 of the Polish State Committee for Scientific Research.

[1]Present address: Los Alamos National Laboratory, Los Alamos, NM 87545

DISCLAIMER

Chapter 1

HEATING OF NUCLEAR MATTER AND MULTIFRAGMENTATION: ANTIPROTONS VS PIONS

L. Beaulieu[1,*], T. Lefort[1], W.c-Hsi[1], K. Kwiatkowski[1], V.E. Viola[1], L.Pienkowski[2], R.G. Korteling[3], R. Laforest[4], E. Martin[4], E. Ramakrishnan[4], D. Rowland[4], A. Ruangma[4], E. Winchester[4], S.J. Yennello[4], H. Breuer[5], S. Gushue[6], L.P. Remsberg[6], and B. Back[7]

[1] *Department of Chemistry and IUCF, Indiana University, Bloomington IN 47405*

[2] *Heavy Ion Laboratory, Warsaw University, Warsaw, Poland*

[3] *Department of Chemistry, Simon Fraser University, Burnaby, B.C., V5A 1S6, Canada*

[4] *Department of Chemistry and Cyclotron Laboratory, Texas A&M University, College Station, TX 77843*

[5] *Department of Physics, University of Maryland, College Park, MD 20742*

[6] *Physics Division, Brookhaven National Laboratory, Upton, NY 11973*

[7] *Physics Division, Argonne National Laboratory, Argonne, IL 60439*

Abstract Heating of nuclear matter with 8 GeV/c $\bar{p}$ and π^- beams has been investigated in an experiment conducted at BNL AGS accelerator. All charged particles from protons to $Z \simeq 16$ were detected using the Indiana Silicon Sphere 4π array. Significant enhancement of energy deposition in high multiplicity events is observed for antiprotons compared to other hadron beams. The experimental trends are qualitatively consistent with predictions from an intranuclear cascade code.

Keywords: 8 GeV/c π^-, $\bar{p}$+Au, 4π detector, multifragmentation, heating of nuclear matter, event-by-event excitation energy, cascade calculations.

email: LBeaulieu@iucf.indiana.edu
url: http://www.iucf.indiana.edu/~lbeaulieu/

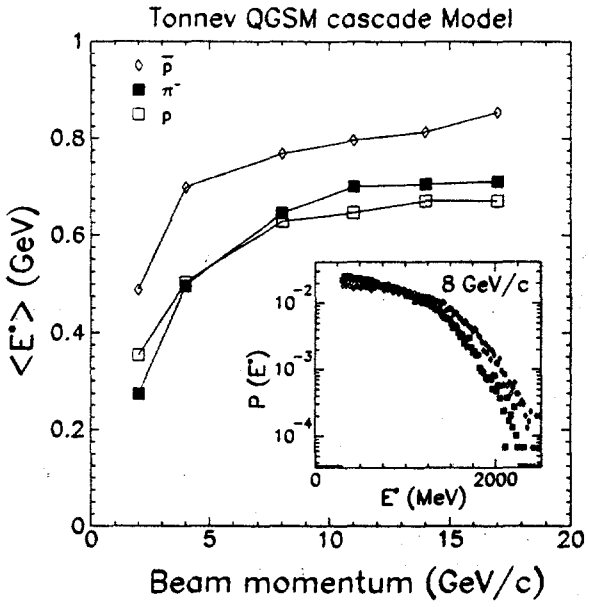

Figure 1.1 Average excitation energy deposited by $\bar{p}$, π^- and p beams as a function of beam momentum as predicted by a cascade code [12]. The insert shows the predicted excitation energy distributions for $\bar{p}$ and π^- beams at 8 GeV/c.

1. INTRODUCTION

The "quest" for the liquid gas phase transition in nuclear matter using heavy ion collisions at intermediate energies has been punctuated by heated debates in recent years, ranging from the very small cross section for fusion of the two partners [1, 2] to the dominance of dynamical effects [3-8] over thermal equilibrium [9].

In the midst of such complexities, the use of GeV hadron projectiles impinging on nuclei offer many unique advantages in producing highly excited nuclear matter. Hard N-N scattering leads to a very efficient and fast ($\leq$ 30-40 fm/c) heating of the target nuclei via excitation of Δ(N*) resonances and pion reabsorption [10, 11]. Moreover, hadron beams impart little compression and angular momentum to the excited nuclei. Therefore, any futher decay of the (single!) excited source should be dominated by thermal effects.

Of all the hadron projectiles, the antiproton beams are expected to offer a significant enhancement of the excitation energy deposition relative to other hadrons, while retaining the same simplicity of the reaction dynamics described previously. This enhancement is related to the probability for reabsorption of the large number of pions created by

the annihilation process ($n_\pi \simeq 5$). This effect is illutrated in Fig. 1.1, using Toneev's QGSM cascade code [12], which shows the average excitation energy imparted to the nuclei as function of beam momentum for protons, pions and antiprotons. The enhancement of excitation energy predicted for antiproton beams is on the order of 30%.

For all beams, a saturation of energy deposition is seen at high beam momentum due to a decreasing probability for nuclear stopping. The saturation of energy deposition has been seen experimentally in ^{3}He-induced reactions at around 5 GeV kinetic energy [13], and also in pion- and proton-induced reactions from 5 GeV/c to 14.6 GeV/c [14]. Futhermore, Hsi et al. [14] have observed very regular behavior of various experimental distributions and averages, leading to conclusion that 5 GeV/c pion-induced reactions produce a thermal source with essentially the same characteristics as 14.6 GeV/c proton-induced reactions on the same target. This constitutes an experimental verification that pion- and proton-induced reactions have the same heating "efficiency" as shown on Fig. 1.1.

Based of previous results and the cascade predictions, the antiproton-nucleus reactions would be expected to yield a data set that spans the complete rise of multifragmentation and extend into the vaporization regime (fall of multifragmentation) [15]. In the following, a comparison of the heating efficiency of pions versus antiprotons at the same beam momentum will be presented.

2. EXPERIMENT

Experiment E900a was performed at the Brookhaven National Laboratory AGS accelerator. Negative secondary beams consisting of pions, kaons and antiprotons were tagged with a time-of-flight/Cerenkov counter system. The time-of-flight consisted of a 12 mm thick Bicron 480 scintillator start detector followed, 64 meters downstream, by a 5mm thick Bicron 418 scintillator stop detector. Clean separation between $\bar{p}$ and π^- projectiles was achieved with a timing resolution of 200 ps (standard deviation). Negative pions overlapping with $\bar{p}$ were identified and vetoed using a 7 m CO_2 Cerenkov counter operated at atmospheric pressure. The purity of the beam at the target is 98% π, $\sim$ 1% $\bar{p}$ and $\sim$ 1% K^-. The identification of K^- remains a difficult task even after veto of negative pions.

Beams consisting of $\approx 4\times10^6$ particle/spill (4.5 s spill time, $\approx$ 2.2 s flat top) were incident on a 2×2 cm^2 self-supporting 2mg/cm^2 thick ^{197}Au target. The target was suspended on two 50 μm tungsten wires to reduce halo reactions. Charged particles from the π^-, $\bar{p}$+Au reactions

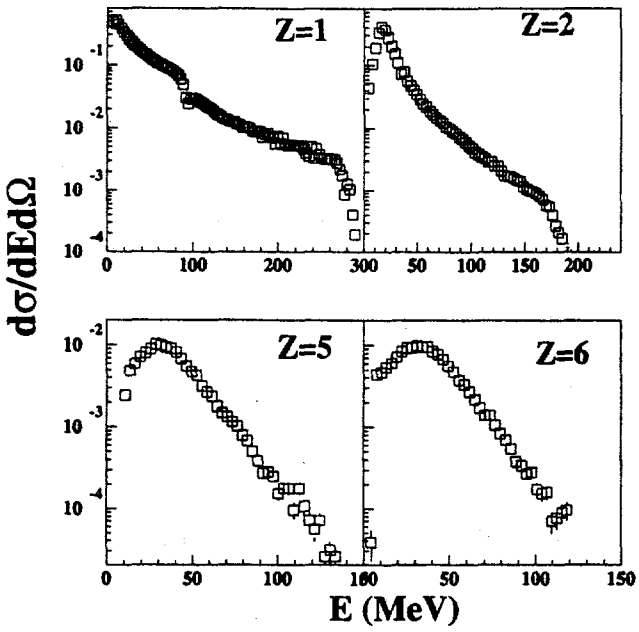

Figure 1.2 Kinetic energy spectra in the laboratory frame for Z=1, 2, 5 and 6 measured between 128° and 147°.

were measured with the ISiS 4π array consisting of 162 triple telescope detectors covering 74% of the 4π solid angle between 14^o and 166^o [16]. Each telescope is made of an ion chamber (IC), 500 μm Si and 2.8 cm CsI(Tl) crystal read by a photodiode. The first stage (IC-Si) provides elemental charge resolution up to $Z \simeq 16$ for kinetic energies between 0.7 to 8 MeV/nucleon. Mass and charge resolution is achieved in the second stage (Si-CsI) for hydrogen, helium and lithium with kinetic energies between 8A MeV to 92A MeV. Unidentified ("grey") charged particles, mainly protons, up to about 300MeV are also detected.

The trigger for this experiment was a fast signal in at least three Si detectors. Acquisition was permitted only during the flat top period of the spill. This is reflected in our software requirement of having 3 or more detected charged particles. Additional software cuts required the kinetic energy of Z=1 to 5 fragments to be greater than 1 MeV/nucleon, and at least one fragment ($Z \geq 3$) or one helium must be detected in the IC-Si stage. These last cuts were made to reduce noise. The final event sample is made of 25 000 $\bar{p}$ and 2 500 000 π^-.

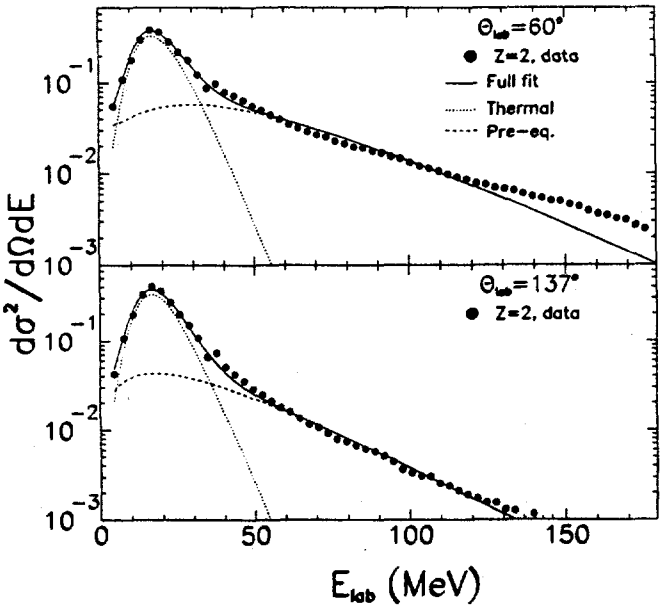

Figure 1.3 Moving source fits on the helium kinetic energy spectra at forward angles (top panel) and backward angles (bottom panel). The dotted line corresponds to the thermal source fit, and the dashed line to the pre-equilibrium component. The full curve is the sum of the thermal and pre-equilibrium fits

3. "UNPROCESSED" RESULTS

Laboratory energy spectra for hydrogen, helium, boron and carbon fragemnts measured between 128° and 147° are shown in Fig. 1.2. The spectra for the heavier fragments peak roughly at the Coulomb barrier (or slighly lower) and can be characterized by a single slope, reminiscent of emission from a single thermalized source. Light charged particles have a dominant thermal component at low kinetic energies but clear deviation is seen at higher energies. The contribution of high energy non-equilibrium particles is larger at forward angles, and is also present for light fragments (Z=3-4).

Two moving source fits, using Moretto's formalism [17], yield very good reproduction of the helium energy spectra at backward angles (Fig. 1.3, bottom panel). At forward angles (Fig. 1.3, top panel), the thermal source is well described but not the high energy tails, which require a much flatter slope beyond 100 MeV of kinetic energy. These particles probably come from the early time of the reactions and are related

to the initial knock-out ("splash") of nucleons by the primary projectile. They constitute a measure "centrality", as defined in ref. [18]. The parameters of the thermal source, deduced from the helium energy spectra, are: T_{th}=4.8 MeV and V_{th}=0.0012c. Notice the very small source velocity for the thermal component.

The separation of the thermal source from the preequilibrium contributions is achieved by selecting the particles based on their kinetic energy in the source frame (E_{cm}), assuming that the source velocity of 0.0012c is along the beam axis. This selection makes use of the experimental systematic analysis of the ^{3}He-induced reactions between 1.8 GeV and 4.8 GeV [19, 20]:

$$E_{cm} \leq 9.0Z + 40MeV \quad ; Z \geq 2 \tag{1.1}$$

$$E_{cm} \leq 30MeV \quad ; Z = 1 \tag{1.2}$$

The effectiveness of the method was tested by constructing the angular distribution of the selected thermal particles, and verifying that it has the expected feature of an isotropic source [21].

Our hability to isolate a single thermal component combined with very small collective effects for this reaction, open the possibility of extracting the source temperature using Maxwell-Boltzmann fits to the energy spectra [22]. Comparison of the kinetic thermometer in such a simple scenario to the isotope ratios thermometer [23, 24] should bring new insights to the temperature measurement problems [25].

3.1 ANTIPROTONS VS PIONS

Any enhancement of energy deposition using $\bar{p}$ instead of π^- projectiles should be seen in "raw" global variables to be of significant interest. This first point was tested by looking at the probability distributions of the observed multiplicity of charged particles (N_c), the observed multiplicity of fragments (N_{imf}) and the transverse energy of all charged particles, defined by $E_t = \sum_{i=1}^{N_c} E_i sin^2\Theta_i$. These probability distributions, shown on the top panels of Fig. 1.4, exhibit a strong enhancement in favor of the $\bar{p}$ projectiles for the last 15-20% of the observed cross-section (from N_c and E_t). These events are expected to correspond to high excitation energy events, and are possibly the best candidates for observing phase transition-like behavior [20].

The enhancement is quantified in the bottom panels of Fig. 1.4 by taking the ratios of the above probabilities, $P(\bar{p})/P(\pi^-)$. As stated before, most of the emitted IMFs come from the thermal source, and should be examined at first. The increase in probability is about 80% for 5 IMF events. On the other hand, the ratio for N_c is even stronger going up to

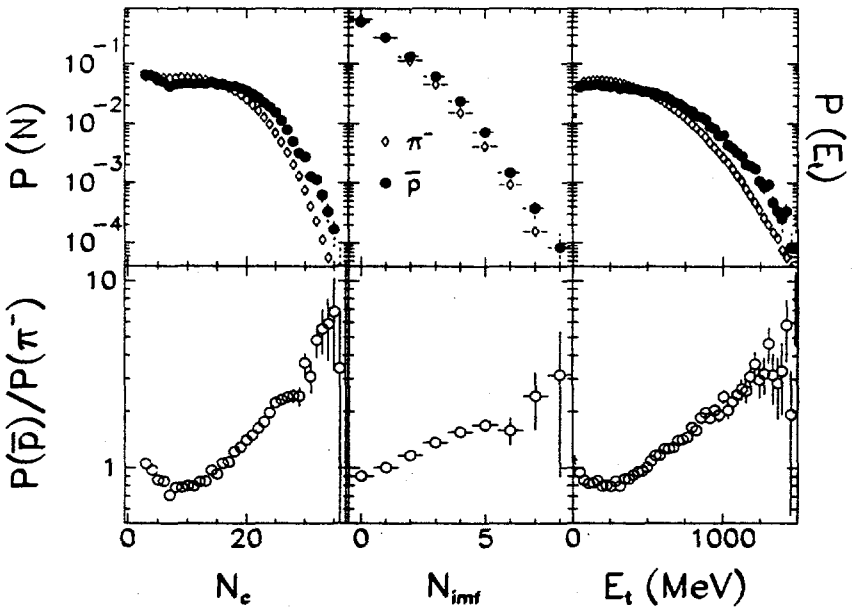

Figure 1.4 Top panels: Probability distributions for the observed charged-particle (left) and IMF multiplicities (middle), and for the total transverse energy (right). The open and black symbols are for pion and antiproton beams, respectively. Bottom panels: Ratio of the $\bar{p}$ to π^- probability distributions of the corresponding global variable from the top panels.

a factor of 8 for the largest multiplicities. The probability ratio for E_t is somewhat between these two extremes showing a four-fold increase. All three observables show signs of a significant enhancement of energy deposition with $\bar{p}$ projectiles. The difference between N_c and N_{imf} could be interpreted as a signature that the decay mechanism is favoring more the light charged particles than the IMFs. This would mean that the hot source has enter the vaporization regime. However, these are observed multiplicities, and therefore include fast particles. A separation of the multiplicity in term of fast and thermal gives an increase of about 300-400% for the fast particles but only a 100% for the thermal source. Therefore, the increase of thermal charged particle multiplicity follows closely that of the IMF to first order (cf. Fig. 1.4). The immediate implication is that the observed increases are partially due to fast/non-equilibrium emission of light charged particles $Z \leq 2$. This gives a rough idea of how the annihilation energy is divided among the thermal and non-thermal components, and invites comparisons to models in order

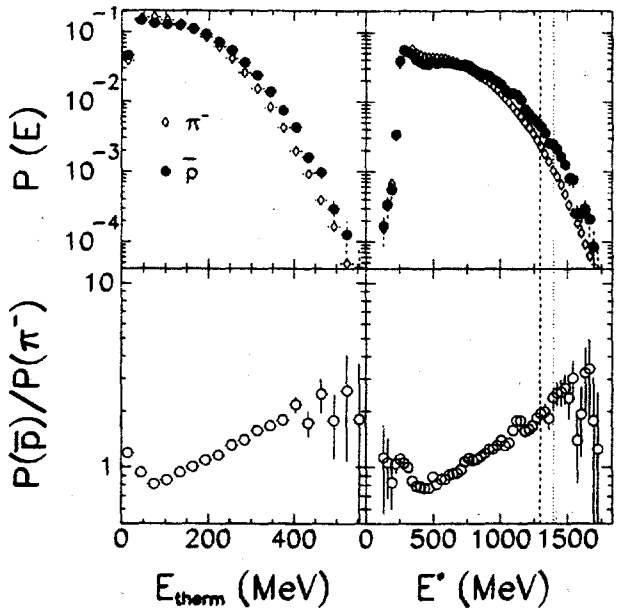

Figure 1.5 Thermal kinetic energy (top left) and thermal excitation energy (top right panel) distributions for pions and antiprotons beams. Bottom panels: Ratio of the $\bar{p}$ to π^- probability distributions of the corresponding global variable from the top panels. The dashed and dotted vertical lines represent the last 1% of the excitation energy distribution for pions and antiprotons respectively.

to extract the details. Since E_t is constructed from all the observed charged particles, the same interpretation as for N_c applies. To be more quantitative, it is necessary to construct observable sensitive only to the thermal excitation energy.

4. "MASSAGE" RESULTS

The kinetic energy of all thermal particles, selected according to Eq. 1.1-1.2, are used to construct the total thermal energy, E_{therm}. The probability distribution of E_{therm} in Fig. 1.5 indicates an increase in cross-section at larger thermal energies for $\bar{p}$ compared to π^- beams. The enhancement is about a factor of 2 at the highest value of E_{therm}.

Going from thermal energy to excitation energy requires several assumptions [20]. Each event is separated into two groups: fast and thermal particles. The excited residue (primary source after non-equilibrium

emission) mass and charge are obtained by subtracting all the fast particles from the target mass and charge

$$A_{res} = A_{tgt} - \sum A^{fast} - \sum M_n^{fast} \tag{1.3}$$

$$Z_{res} = Z_{tgt} - \sum Z^{fast} \tag{1.4}$$

Corrections for geometrical efficiency are taken into account. The multiplicity of fast neutrons, M_n^{fast} is taken to be $1.93 \times M_p^{fast}$, where M_p^{fast} corresponds to the efficiency-corrected experimental multiplicity of fast protons ($E_{cm} > 30$ MeV). This procedure to estimate the fast neutrons is intermediate between the experimental low-energy systematics of Polster et al. [26] and that expected from INC calculations [27].

For thermal particles, the kinetic energy of each particle in the source frame (K_i) is computed. The multiplicity of thermal neutrons, M_n, is obtained using the measured multiplicity of thermal charged particles M_c according to the experimental work of Goldenbaum and co-workers [28]. Again, corrections for geometrical efficiency was made on all observables related to the detected charged particles. The excitation energies E^* were assigned on an event-by-event basis according to the following prescription

$$E^* = \sum_{i=1}^{M_c} K_i + M_n \langle K_n \rangle + Q + E_\gamma \tag{1.5}$$

E_γ is taken to be $1 \times (M_c + M_n)$ MeV. The reconstructed event is used to determine the mass difference Q. $\langle K_n \rangle$ is assigned a value of $3T/2$ where $T = \sqrt{E^*/a}$ and $a = A_{res}/11$ MeV^{-1}, and then iterated to obtain a self-consistent value. It should be stressed that this procudere was appplied the same way to both the $\bar{p}$ and the π^- beams.

The excitation energy distributions are presented in Fig. 1.5 (right panels). The increase of excitation energy imparted to the target nuclei using $\bar{p}$ projectiles is consistent with that of the thermal energy on the left panels with almost a factor 2 more cross-sections at high excitation energies. The dashed and dotted lines correspond to the last 1% of the observed cross-sections (roughly 10-20 mb) for π^- and $\bar{p}$, respectively. This translates in an increase of the maximum excitation energy of 1.3 MeV/nucleon using $\bar{p}$ beams (last 1% is 9.0 MeV/nucleon for π^- and 10.3 MeV/nucleon for $\bar{p}$). This is in qualitative agreement with QGSM code as shown in Fig. 1.1 (see insert).

The excitation energy and residue mass distributions are compared directly to the QGSM cascade code in Fig. 1.6, using the default values for the various parameters. The excitation energy distributions predicted

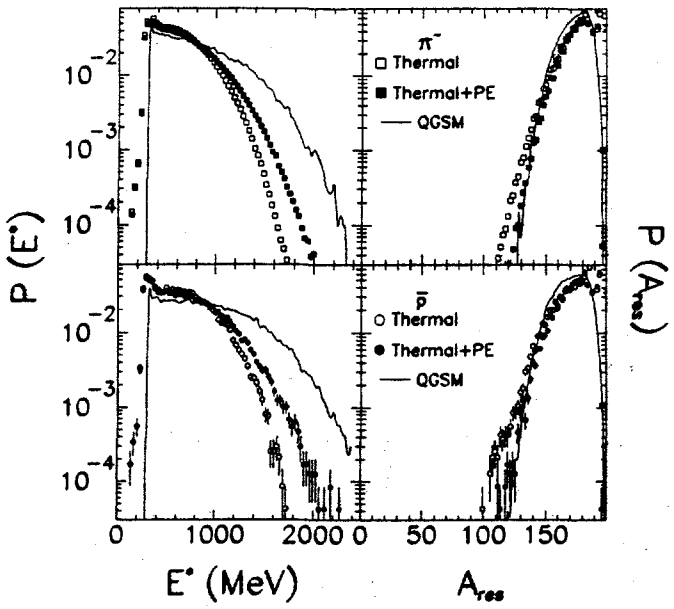

Figure 1.6 Excitation energy and residue mass distributions for pions (top panels) and antiprotons (bottom panels) obtained using Eq. 1.1-1.2 (open symbols) and an extension to 30 MeV/nucleon of kinetic energy for thermal particles (black symbols). See text for details. The curve correspond to the prediction of Toneev's QGSM cascade code [12].

by QGSM reach higher values than the data for both beams while A_{res} tend to be slightly bigger. A possible explanation may be the use of a too high cut-off energy for nucleons to escape during the cascade, trapping more particles and increasing E^* and A_{res}. To verify this hypothesis, the excitation energies were re-evaluated by relaxing the definition of thermal particles to include all particles with kinetic energies smaller than 30 MeV/nucleon, thus including some non-equilibrium particles. The result of this exercise is shown in Fig. 1.6 as the black symbols. A_{res} probability distributions are now in good agreement with Toneev's QGSM but the code still predicts more excitation energy than the data. Therefore, a more important effect than the nucleon escape energy cut-off might be the pion reabsorption cross-section or other cross-sections related to pions and resonances used in the code.

5. SUMMARY

Heating of nuclear matter has been investigated using $\bar{p}$ and π^- projectiles at 8 GeV/c beam momentum. The raw multiplicity distributions, N_c and N_{imf}, the transverse and the thermal energy distributions show significant enhancement of energy deposition with $\bar{p}$ beams relative to other hadrons. Separation of thermally emitted particles from preequilibrium ones was performed on the kinetic energy spectra. The primary residue mass and excitation energy distributions were reconstructed event-by-event for both beams under consideration. The increase in cross-section for high excitation energy events reaches 100% with $\bar{p}$. The excitation energy distribution for antiprotons reaches higher values (1.3 MeV/nucleon higher) than for pions as measured by the last 1% of their respective distributions. The results are in qualitative agreement with a cascade code but the code overpredicts the absolute values. The enhancement of thermal energy deposition is also accompanied by a stronger increase of fast proton and light cluster emission, and should be related to the details of the annihilation process itself. Certainly, an in-depth comparison to models is needed to shed light on the energy deposition in this beam momentum region.

Acknowledgments

The authors wish to thank John Vanderwerp, Bill Lozowski and Dick Yoder at IUCF and Phil Pile, Joe Scaduto, Larry Toler, John Gould and Jerry Bunce at AGS for their assistance with the experiement. This work was supported by the US Department of Energy and the National Science Foundation, the National Sciences and Engineering Research Council of Canada and the Robert A. Welch Foundation.

References

[1] J. Péter *et al.*, (1995) Nucl. Phys. **A593**, 95.

[2] L. Beaulieu *et al.*, (1996) Phys. Rev. Lett. **77**, 462.

[3] C.P. Montoya *et al.*, (1994) Phys. Rev. Lett **73**, 3070.

[4] J. Lukasik *et al.*, (1997) Phys. Rev. C **55**, 1906.

[5] Y. Larochelle *et al.*, (1997) Phys. Rev. C **55**, 1869.

[6] J. Toke *et al.*, (1995) Phys. Rev. Lett. **75**, 2920.

[7] J.F. Lecolley *et al.*, (1995) Phys. Lett. B **354**, 202 .

[8] J.F. Dempsey *et al.*, (1996) Phys. Rev. C **54**, 1710.

[9] L.G. Moretto, *et al.*, Phys. Rep. **287**, 249 (1997), and references therein.

[10] G.Wang *et al.*, (1996) Phys. Rev. C **53**, 1811.

[11] J. Cugnon *et al.*, (1987) Nucl. Phys. **A470**, 558, (1989) Ann Phys. (Paris) **14**, 49.

[12] V. Toneev *et al.*, (1990) Nucl. Phys. **A519**, 463.

[13] K.B. Morley *et al.*, (1995) Phys. Lett. **B 355**, 52.

[14] W-c. Hsi, *et al.*, (1997) Phys. Rev. Lett. **79**, 817.

[15] C.A. Ogilvie, *et al.*, (1991) Phys. Rev. Lett. **67**, 1214.

[16] K. Kwiatkowski *et al.*, (1995) Nucl. Instr. Meth. **A360**, 571.

[17] L.G. Moretto, (1975) Nucl. Phys. **A247**, 211.

[18] R. Soltz *et al.*, Contribution to these proceedings; I. Chemakin *et al.*, (1999) submitted to Phys. Rev. C and nucl-ex 9902003.

[19] D.S. Bracken, (1996) Ph.D. thesis, Indiana University.

[20] K. Kwiatkowski *et al.*, (1998) Phys. Lett.**B 423**, 21.

[21] T. Lefort *et al.*, (1999) Proceedings of the 37th International Winter Meeting on Nuclear Physics, Bormio, Italy, Jan 25-30 1999.

[22] A. Siwek *et al.*, (1998) Phys. Rev. C **57**, 2507.

[23] J. Albergo *et al.*, (1985) Nuovo Cim. **89A**, 1.

[24] J. Pochodzalla *et al.*, Phys. Rev. Lett. **75**, 1040 (1995).

[25] V.E. Viola, K. Kwiatkowski and W.A Friedman, (1999) accepted for publication in Phys. Rev. C.

[26] D. Polster *et al.*, (1995) Phys. Rev. C **51**, 1167.

[27] I.A. Pshenichnov *et al.*, (1995) Phys. Rev. C **52**, 947.

[28] F. Goldenbaum *et al.*, (1996) Phys. Rev. Lett. **77** 1230; L. Pienkowski *et al.*, (1994) Phys. Lett. B **B336**, 147.